Thermal transmittance effect on energy consumption of Mediterranean buildings with different thermal mass

Eugénio Rodrigues[a,*], Marco S. Fernandes[a],
Adélio Rodrigues Gaspar[a], Álvaro Gomes[b], José J. Costa[a]

[a] *ADAI, LAETA, Department of Mechanical Engineering, University of Coimbra, Rua Luís Reis Santos, Pólo II, 3030-788 Coimbra, Portugal*
[b] *INESC Coimbra, Department of Electrical and Computer Engineering, University of Coimbra, Rua Sílvio Lima, Pólo II, 3030-290 Coimbra, Portugal*

Abstract

High thermal mass construction is commonly used to reduce cooling energy consumption during the summer period as a passive design strategy in the Mediterranean region. Although being a generalized design practice, the benefit to the building performance is not fully consensual within the scientific community. This work explores the influence of thermal transmittance on the energy efficiency of buildings with different thermal mass levels. Hence, a statistical comparison of the buildings' annual energy consumption for air-conditioning is carried out based on two synthetic datasets with high and low thermal mass and varying thermal transmittance for opaque and transparent elements. In addition to climate location, the results demonstrate that thermal transmittance has varying impact on the contribution of thermal mass. The locations presenting such behavior were Marseille (−0.99 % to +3.89 %), Istanbul (−0.73 % to +4.21 %), Valencia (−1.31 % to +4.97 %), Algiers (−2.32 % to +3.81 %), Malaga (−3.95 % to +6.21 %), Casablanca (−5.66 % to +6.96 %), and Tel Aviv (−1.81 % to +5.44 %). These findings demonstrate that the influence of thermal mass is more complex than previously thought and levels should be chosen in relation with the thermal transmittance value.

Keywords: generative design method, dynamic simulation, residential buildings, thermal transmittance, thermal mass, Mediterranean climates

1. Introduction

When designing new buildings, geometry and construction play an important role in achieving high energy performance. For this reason, researchers are studying the best passive measures to be considered at the design phase. One of the measures is the use of adequate thermal mass construction, which can contribute to reduce the indoor air temperature fluctuations [1], thus

*Corresponding author.
Email address: erodrigues@uc.pt (Eugénio Rodrigues)

diminishing the use of active systems during hot days [2, 3]. However, thermal mass may also have the undesired effect of requiring anticipated heating or cooling to reach the air-conditioning setpoints in time, thus increasing energy consumption, and possibly thermal discomfort.

Despite the widespread idea among building design practitioners that heavyweight construction is beneficial to reduce energy consumption, studies are not conclusive, especially due to current thick insulation requirements in the buildings' envelope imposed by energy saving standards [4]; therefore, this is still an open question [5].

According to the review article by Verbeke and Audenaert [6] on thermal inertia in buildings, the reasons for the variability in the studies' findings are i) the different climate conditions, ii) the lack of common metrics for describing thermal inertia, iii) the use of different methodologies, iv) the different parametrization and settings in studies that use building energy performance simulation, v) the different building types among studies, vi) the varying definitions of both 'optimal' thermal mass and 'energy use' goal, and vii) several studies focus only on the individual building elements and not on the whole building. The same authors also point out that the reviewed studies neglect the contribution of the buildings' interior partitions and furnishings. Since the studies focus on a single building (or on a small set of buildings) for a specific weather location, findings cannot be generalized, as they are limited to a climate location and buildings can have different functions, forms, indoor arrangements, construction, and occupation.

Studies for the warm and mild climates of the Mediterranean region present diverse results. Aste et al. [7] carried out a parametric study to compare the effects of two exterior wall types (high and low thermal inertia) having the same U-value ($0.34\,\mathrm{W \cdot m^{-2} \cdot K^{-1}}$) on energy performance for the climate conditions in Milan, Italy. The study revealed that low thermal inertia walls increased energy demand for heating by up to 10 % and up to 20 % for cooling. The authors also noticed that the influence of the thermal inertia of the exterior walls depended significantly on the design and operational parameters of the building's air-conditioning. However, in a more recent study, Aste et al. [8] carried out a parametric study on office buildings located in Milan, Rome and Palermo (Italy), to determine the sensible heating and cooling demands and compare the thermal capacity of exterior walls, roofs, and floors elements with medium-heavy, medium, and light thermal mass. The authors concluded that medium-heavy configurations evidenced lower energy demand only if adequate night ventilation was used.

Similarly, Stazi et al. [9] found that even though thermal mass had little influence on energy savings, it had a major impact on comfort levels. The study evaluated the energy, comfort and environmental impact of three construction types (wood, wood-cement, and masonry) in Ancona, Bolzano, Palermo (Italy), London (UK), and Cairo (Egypt). Winter and summer seasons were analyzed in semi-stationary and dynamic conditions. The authors recommend thick insulation and

high internal mass for low-energy buildings in Mediterranean climates. More recently, Stazi et al. [10] conducted an experimental study to determine the combined effect of the internal areal heat capacity and the decrement factor (ratio of the modulus of the periodic thermal transmittance to the steady-state thermal transmittance) in an on-site test room without windows and a high thermal insulation level. The tests were carried out in Agugliano (Italy) during summer and winter seasons. According to the authors, the solution that presented the best performance on an annual basis had medium thermal inertia properties ($33\,\mathrm{kJ \cdot m^{-2} \cdot K^{-1}}$ and 0.072 for internal areal heat capacity and decrement factor, respectively).

In cold climates, studies also display some conflicting results. For example, Dodoo et al. [11] concluded that in colder regions the benefit of high thermal mass is negligible. The authors studied a 4-story residential building with 16 apartments, which was dynamically simulated with two construction systems (concrete *vs.* wood-frame), in three locations in Sweden. The results revealed that high thermal mass construction only benefited from a decrease in heating demand ranging from 0.5 % to 2.4 %, depending on the tested location. Reilly and Kinnane [12] studied heating energy consumption in Belfast (Ireland) using a newly developed metric and concluded that heavyweight walls increased energy consumption, in comparison to lightweight walls.

In extreme desert climates, the studies seem to converge to the conclusion that high thermal mass contributes to improving the building's performance. Gregory et al. [13] numerically determined the impact of the thermal mass of four different exterior walling systems with the same R-value of $1.5\,\mathrm{m^2 \cdot K \cdot W^{-1}}$ on the thermal performance of four simplified building models (single-zone) in Australia. The authors concluded that thermal mass has a dramatic impact on thermal behavior, particularly in the models with thermal mass on the inner side of the insulation layer and that buildings with larger windows require larger amount of thermal mass, proportionally. Zhu et al. [14] monitored the thermal energy transmitted through the exterior walls of two identical houses, placed side-by-side in Las Vegas (USA) but having different construction characteristics: a concrete/insulation wall-sandwich type and a lightweight wood-framed wall type, with similar equivalent R-values of $6.98\,\mathrm{m^2 \cdot K \cdot W^{-1}}$. The collected data was used to implement a dynamic simulation model to predict heating and cooling energy consumption. The authors observed that the heavyweight construction presented a lower heating energy consumption. They also concluded that in desert climates, as the one in Las Vegas, with high outdoor temperatures and high amount of sunlight exposure, this type of wall requires more energy for cooling, as heat is stored and not released to the exterior during the night.

Concerning the influence of the relative positions of mass and insulation, Al-Sanea and Zedan [15] conducted a study on the performance of west-oriented exterior walls in Riyadh (Saudi Arabia), where the positions of thickness-optimized insulation layers (1-, 2-, or 3-layers) were compared

according to the dynamic thermal characteristics of time lag, peak load, and decrement factor. The authors noticed that 2-layered insulation placed in the middle and on the exterior side of the wall and 3-layered insulation walls had the largest time lag, reaching 10 h and 12 h delays, respectively. A 20 % decrease for peak cooling and heating transmission loads was also found. In another study, and based on the same numerical approach, Al-Sanea et al. [16] found that, for exterior walls with the same U-value in Riyadh, insulation provides a better thermal performance when positioned on the outside. The authors also concluded that the maximum annual energy savings for cooling and heating may reach 17 % and 35 %, respectively, for the optimized thermal mass thickness. In line with the same concern to determine the best sequence and distribution of layers in exterior walls, Leccese et al. [17] reached different conclusions by studying different constructive solutions with distinct dynamic thermal performance using the heat transfer matrix method. The results showed that lighter constructions with insulation on both sides of the exterior walls (having a time lag ranging from 8 h to 12 h) are more favorable than heavier solutions.

Thermal inertia is often evaluated according to the admittance procedure reported in the international standard ISO EN 13786 [18]. According to this standard, opaque elements can be characterized through certain dynamic parameters (periodic thermal transmittance, decrement factor and time shift), which can be calculated starting from the component's materials' thermal properties. However, when the assumptions about heat flux are not met, or the material thermophysical properties are unknown (*e.g.*, in existing buildings or in exploratory simulation studies), proper accuracy of results is not ensured, or the method is not even applicable. In those cases, simplified criteria are often applied, for example by roughly describing the thermal inertia influence recurring to the useful thermal mass or an approximated value of the time constant [7]. This approach, which is still reflected in some national regulations on energy saving in buildings, appears to be insufficient in many cases, but it can lead to some general useful indicators (that may help in more specific studies). Further details on this subject can be found in Bishara et al. [19], where both experimental and numerical tests to assess the impact of different sources of uncertainty on the estimation of ISO EN 13786 dynamic parameters are presented.

The present work is devoted to studying the impact of thermal mass and its relation with the thermal transmittance value on the energy performance of a building, calling into question the choice of the most suitable thermal mass level is determined only by the climate type. This study overcomes the issues pointed out by Verbeke and Audenaert [6] by statistically comparing two synthetic datasets of detailed single-family dwellings, having different thermal mass construction, in sixteen locations in the Mediterranean region. Each dataset is constituted by information collected from buildings that are randomly created using a generative design method [20–22] and evaluated through dynamic simulation (EnergyPlus v8.8.0) [23, 24]. In addition to different geometries, the

generated buildings also have random pairwise values of thermal transmittance for the opaque and transparent elements of the building envelope. This approach of generating synthetic datasets was used in the past to study the relevance of geometry-based indexes as thermal performance indicators [25]; to determine the impact of thermal transmittance variation in building design practice in eight climate regions in Europe [26]; to find the most adequate thermal transmittance values for heavyweight construction in sixteen locations in the Mediterranean region [27]; and to foster lightweight steel-framed construction in hot arid climates [28].

The paper is divided into four main sections: the current one (Introduction), followed by the Methodology, Results and Discussion, and finally, the Conclusion.

2. Methodology

To test the impact of the construction's thermal mass on the building's energy performance, a three-step methodology was used for each of the two thermal mass levels. In the first step, a generative design method was used to produce alternative building solutions, which satisfy the same geometric and topologic requirements. For each Mediterranean location, 12 000 two-story residential buildings were randomly generated having random thermal transmittance values for the opaque and transparent envelope elements. In the second step, dynamic simulation was used to assess the buildings' annual energy demand for air-conditioning. The buildings' geometry data, performance evaluation, and construction specifications were stored as two datasets, one for each thermal mass level. Lastly, in the third step, a statistical analysis of the datasets was carried out to compare the impact of the different construction mass levels in small residential buildings.

The dataset of heavyweight construction was used to determine the most adequate thermal transmittance values in ref. [27]. Therefore, this work only examines the lightweight construction dataset in detail and compares it with the heavyweight construction dataset.

2.1. Generative design method

To create alternative building geometries that satisfy the same initial preferences and requirements, the Evolutionary Program for the Space Allocation Problem (EPSAP) algorithm [20–22] was used. The algorithm finds the indoor floor plan layout for each story according to geometric and topologic specifications for each space and opening. In the case of this study, the building specifications correspond to a two-story family house (the same as in ref. [27]) with a hall, a living room, a kitchen, a bathroom and a stair in the ground floor level, and a corridor, a master bedroom, a double bedroom, a single bedroom and a second bathroom in the upper floor (see Table 1 for the complete requirements for each space). Each space has its type defined (circulation, service, or living), relative importance (ranks the importance of each space in comparison to the

remaining spaces from none to max), stories that it serves, minimum space floor side dimension, minimum space floor area, and ratios for the space floor sides. Each space may have one or more exterior openings (see Table 2), by specifying the opening type (door, gate, or window), minimum width, minimum height, and relative vertical position of the opening to the story floor level. The geometry of the interior openings is also specified, in addition to their adjacency relations between contiguous spaces (see Table 3).

Table 1. Geometry specifications for the different spaces.

Space	C^{sn}	C^{sf}	C^{ri}	C^{sl}	C^{su}	C^{ss} (m)	C^{sa} (m^2)	C^{ssr}	C^{slr}
S_1	Hall	Circulation	Min	L_1	L_1	2.70	10.0	{2.0, 3.0}	{3.0, 1.5}
S_2	Living room	Living	Max	L_1	L_1	3.20	–	1.7	2.0
S_3	Kitchen	Service	Mid	L_1	L_1	1.80	–	1.7	2.0
S_4	Bathroom	Service	Min	L_1	L_1	2.20	–	1.7	2.0
S_5	Stair	Circulation	–	L_1	L_2	–	–	–	–
S_6	Corridor	Circulation	None	L_2	L_2	1.40	6.0	{2.0, 3.0}	{3.0, 1.5}
S_7	Double bedroom	Living	High	L_2	L_2	2.70	–	1.7	2.0
S_8	Main bedroom	Living	High	L_2	L_2	2.70	–	1.7	2.0
S_9	Single bedroom	Living	Mid	L_2	L_2	2.70	–	1.7	2.0
S_{10}	Bathroom	Service	Min	L_2	L_2	2.20	–	1.7	2.0

C^{sn} – name, C^{sf} – function, C^{ri} – relative importance, C^{sl} and C^{su} – served lower and upper stories, C^{ss} – minimum side, C^{sa} – minimum area, C^{ssr} and C^{slr} – space small side and large side ratios

Table 2. Geometry specifications for exterior openings.

C^{os}	Opening	C^{oet}	C^{oew} (m)	C^{oeh} (m)	C^{oev} (m)
S_1	Oe_1	Door	1.00	2.00	0
S_2	Oe_2	Window	2.80	2.00	0
S_3	Oe_3	Window	1.20	1.00	1.00
S_4	Oe_4	Window	0.60	0.60	1.40
S_5	Oe_5	Window	0.80	1.40	0.80
S_6	–	–	–	–	–
S_7	Oe_6	Window	1.80	1.00	1.00
S_8	Oe_7	Window	1.80	1.00	1.00
S_9	Oe_8	Window	1.20	1.00	1.00
S_{10}	–	–	–	–	–

C^{os} – space, C^{oet} – opening type, C^{oew} – minimum width, C^{oeh} – minimum height, C^{oev} – vertical position

Table 3. Geometry and topologic specifications for interior openings.

Opening	C^{oit}	C^{oia}	C^{oib}	C^{oiw} (m)	C^{oih} (m)	C^{oiv} (m)
Oi_1	Door	S_1	S_2	1.40	2.00	0
Oi_2	Door	S_1	S_3	0.90	2.00	0
Oi_3	Door	S_1	S_4	0.90	2.00	0
Oi_4	Door	S_5	S_1	0.90	2.00	0
Oi_5	Adjacency	S_2	S_3	0	–	–
Oi_6	Door	S_5	S_6	0.90	2.00	0
Oi_7	Door	S_6	S_7	0.90	2.00	0
Oi_8	Door	S_6	S_8	0.90	2.00	0
Oi_9	Door	S_6	S_9	0.90	2.00	0
Oi_{10}	Door	S_6	S_{10}	0.90	2.00	0

C^{oit} – type, C^{oia} – opening's space, C^{oib} – destination space, C^{oiw} – minimum width, C^{oih} – minimum height, C^{oiv} – vertical position

The EPSAP algorithm produces a user specified number of solutions by satisfying all the specifications in an evolution strategy approach, where the traditional mutation operator is replaced by transformation operations that perform geometric actions, such as translation, rotation, stretching, mirroring, etc. The algorithm minimizes a weighted-sum cost function of seventeen penalty

functions that evaluate the layout of the gross and construction area, story gross area, floor plan compactness, floor plan overflow, circulation space area, spaces' connectivity, overlapping, fixed position, dimensions and relative importance, opening accessibility, as well as dimensions, overlapping, orientation, and fixed position of openings.

2.2. Building performance evaluation

After each EPSAP algorithm run, the building's performance evaluation was carried out using a coupled dynamic simulation engine [23, 24]. The EnergyPlus (version 8.8.0) software was used for a detailed multi-zone energy performance assessment, considering a yearly period. The 'Conduction Transfer Function' method was selected as the heat balance algorithm for calculating the performance of the building's surface assemblies. This method evaluates the surface heat fluxes linearly and the thermal energy storage phenomena [29]. It is widely used in similar simulation problems and requires a smaller computational time when compared to other algorithms, which is a critical factor in face of the size of the current work's datasets. The selected time step for simulation was 15 min. The surface convection models used in the algorithm for the interior and exterior surfaces of the buildings' envelope were the 'TARP' and 'Adaptive Convection Algorithm', respectively. The 'Full Exterior with Reflections' method was selected as the algorithm for solar distribution, in order to take into account shadow patterns on exterior surfaces caused by shading and the exterior surfaces of all surrounding zones. The selected method for shadow estimation was the 'Average Over Days In Frequency' method, as detailed shadow calculations were not required [30]. The geometric input requirements are related to each EPSAP algorithm run, as referred in Rodrigues et al. [23, 24], while the construction, internal thermal gains and HVAC input specifications are described below. In the scope of this work, the outputs are mainly related with thermal energy demand; *i.e.*, the total, heating and cooling energy consumptions for each one of the buildings' zones. The remaining details regarding the EnergyPlus model can be found in the set of input data files (see ref. [31]).

2.2.1. Construction system

Due to the nature of this study, the building's exterior opaque elements have the same thermal mass and randomly assigned pairwise values of thermal transmittance. Therefore, it is not possible to define their dynamic properties, thus preventing the overall application of the admittance method of ISO EN 13786. Hence, the thermal mass ($\mathrm{kg \cdot m^{-2}}$) is used here as a rough description of the thermal inertia influence, with the light- and heavyweight construction types corresponding to low and high thermal mass values, respectively.

For each thermal mass level to be studied, the construction system has shared elements with fixed thermophysical properties, such as the ground floor and the interior door (see Table 4), and

specific elements with corresponding thermal mass, such as the interior wall and the slab (see Table 5). The exterior opaque elements (walls, roofs, and suspended slabs), except for exterior doors, have the same thermal mass as the interior slab element of the corresponding thermal mass level, while their thermal transmittance is randomly changed throughout the simulations from $0.05\,\mathrm{W\cdot m^{-2}\cdot K^{-1}}$ to $1.25\,\mathrm{W\cdot m^{-2}\cdot K^{-1}}$, in steps of $0.05\,\mathrm{W\cdot m^{-2}\cdot K^{-1}}$. The same U-value is also used for the exterior doors. A constant solar heat gain coefficient (SHGC) of 0.6 is considered for the exterior transparent elements and the variable U-values are proportionally paired with those of the opaque elements, from $0.2\,\mathrm{W\cdot m^{-2}\cdot K^{-1}}$ to $5.0\,\mathrm{W\cdot m^{-2}\cdot K^{-1}}$, in steps of $0.2\,\mathrm{W\cdot m^{-2}\cdot K^{-1}}$. Table 5 summarizes the thermophysical properties of each element for both thermal mass levels.

Table 4. Building construction elements with fixed thermophysical properties.

Element	**Layer**	**Thick.** (m)	k ($\mathrm{W\cdot m^{-1}\cdot K^{-1}}$)	ρ ($\mathrm{kg\cdot m^{-3}}$)	c_p ($\mathrm{J\cdot kg^{-1}\cdot K^{-1}}$)	U ($\mathrm{W\cdot m^{-2}\cdot K^{-1}}$)	**Mass** ($\mathrm{kg\cdot m^{-2}}$)
Ground floor	Structural layer	0.2	1.73	2245.6	836.8	0.437	509.69
	Insulation layer	0.08	0.04	32.1	836.8		
	Filling layer	0.02	0.8	1600	840		
	Regulation layer	0.01	0.22	950	840		
	Finishing layer	0.02	0.2	825	2385		
Interior door	Finishing layer	0.005	0.2	825	2385	2.009	21.15
	Structural layer	0.03	0.067	430	1260		
	Finishing layer	0.005	0.2	825	2385		

k – thermal conductivity, ρ – density, c_p – specific heat, U – thermal transmittance

Table 5. Building construction elements with variable thermophysical properties.

Mass level	**Element**	**Layer**	**Thick.** (m)	k ($\mathrm{W\cdot m^{-1}\cdot K^{-1}}$)	ρ ($\mathrm{kg\cdot m^{-3}}$)	c_p ($\mathrm{J\cdot kg^{-1}\cdot K^{-1}}$)	U ($\mathrm{W\cdot m^{-2}\cdot K^{-1}}$)	**Mass** ($\mathrm{kg\cdot m^{-2}}$)	**SHGC**
High	Interior wall	Finishing layer	0.02	0.22	950	840	4.499	195.01	–
		Structural layer	0.07	1.73	2243	836.8			
		Finishing layer	0.02	0.22	950	840			
	Interior slab	Finishing layer	0.02	0.22	950	840	2.841	494.12	
		Structural layer	0.2	1.73	2245.6	836.8			
		Regulation layer	0.01	0.22	950	840			
		Finishing layer	0.02	0.2	825	2385			
Low	Interior wall	Finishing layer	0.013	0.25	900	1000	0.763	60.55	–
		Regulation layer	0.012	0.13	650	1700			
		Foam layer	0.002	0.05	30	2400			
		Structural/core layer	0.1	0.11	214.3	656.4			
		Foam layer	0.002	0.05	30	2400			
		Regulation layer	0.012	0.13	650	1700			
		Finishing layer	0.013	0.25	900	1000			
	Interior slab	Finishing layer	0.013	0.25	900	1000	0.425	64.36	–
		OSB layer	0.012	0.13	650	1700			
		Foam layer	0.002	0.05	30	2400			
		Structural/core layer	0.3	0.16	55	561.6			
		Foam layer	0.002	0.05	30	2400			
		OSB layer	0.025	0.13	650	1700			
		Finishing layer	0.01	0.17	1200	1400			
Both	Envelope	Thermal mass equivalent to the interior slab of the same thermal inertia level					RAND$\{0.05, \cdots, 1.25\}$	–	–
	Exterior window	–	–	–	–	–	RAND$\{0.2, \cdots, 5.0\}$	–	0.6

k – thermal conductivity, ρ – density, c_p – specific heat, U – thermal transmittance, SHGC – solar heat gain coefficient

2.2.2. Occupancy, lighting, internal gains, and HVAC

The building is a single-family house occupied by five people. The occupancy patterns and activity levels are based on the building typology (see Table 6 and Fig. 1, which are the same specifications as in ref. [27]).

Table 6. Maximum number of people per zone and correspondent activity levels.

Zone type	**Max number of people**[a]	**Activity level** ($W \cdot person^{-1}$)
Living room	5	110
Bathrooms	1	207
Circulation areas	1	190
Kitchen	2	190
Double/Main bedroom	2	72
Single bedroom	1	72

[a] – Regarding the building inhabitants accessing each zone, and not necessarily the number of occupants simultaneously in the zone. The occupant's distribution is defined together with the proper occupancy schedules.

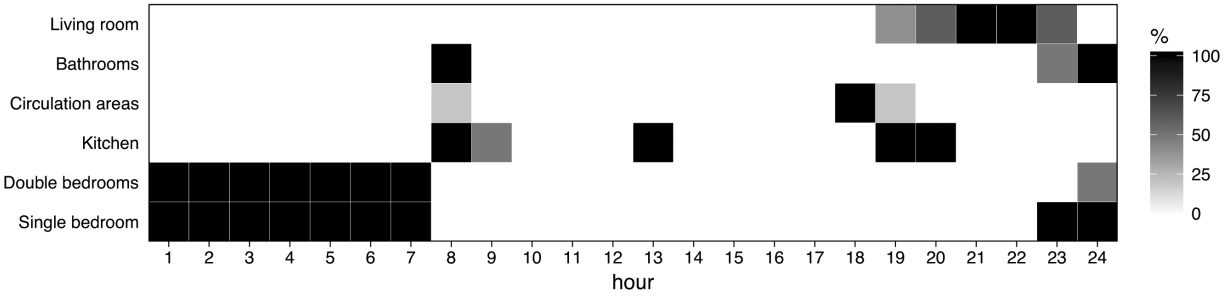

Fig. 1. General occupancy pattern in the building zones.

The design levels and schedules of the lighting and equipment are based on the building's zone typology and occupancy (see Table 7 and Fig. 2, for lighting, and Table 8 and Fig. 3, for equipment, which are the same specifications as in ref. [27]). The lighting schedules are also based on the window shading profiles: PVC roller shutters are assumed to cover all windows during night-time, and daylighting controls are considered to dim the light intensity in spaces with exterior windows, switching them off when daylight illuminance is above 300 lx. This dimming control should be seen here as a "simulation procedure" that allows to adjust the lighting values according to available daylight in each latitude, since the electric lighting profiles are identical in all locations.

Table 7. Maximum design lighting levels for each zone type.

Zone type	**Design lighting level** ($W \cdot m^{-2}$)
Living room/Bedrooms	7.5
Bathrooms	7.5
Circulation areas	3.2
Kitchen	5

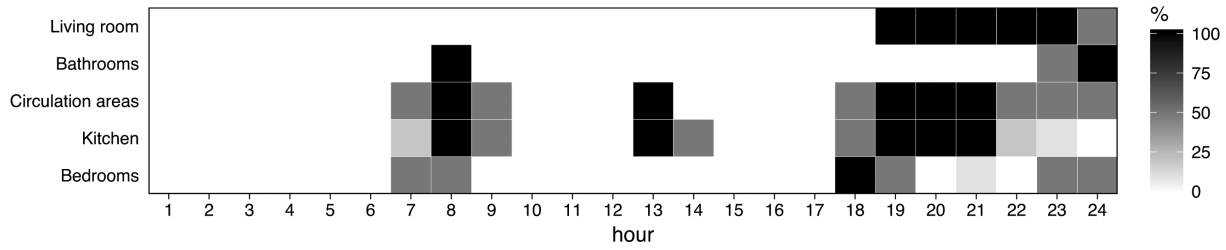

Fig. 2. Electric light schedule in each zone.

Regarding HVAC, the living room and the bedrooms are the only spaces where heating and

cooling are considered. For this purpose, the ideal loads air system model of EnergyPlus is used [30], with the heating/cooling availability schedule for each space defined by the respective occupancy pattern. The indoor temperature thermostat setpoints assumed for cooling and heating are 25.0 °C and 20.0 °C, respectively, for all the case studies. In addition, a 0.6 air change per hour (ACH) exhaust rate is considered for the kitchen and the bathrooms, with a flow rate profile equivalent to the occupancy schedules defined for these spaces, while 0.2 ACH and 0.1 ACH are considered for the outdoor air infiltration into zones with and without exterior openings, respectively.

Table 8. Total heat gains from electric equipment in each zone.

Zone type	**Design level** (W)
Living room	350
Bathrooms	100
Circulation areas	20
Kitchen	1440
Bedrooms	250

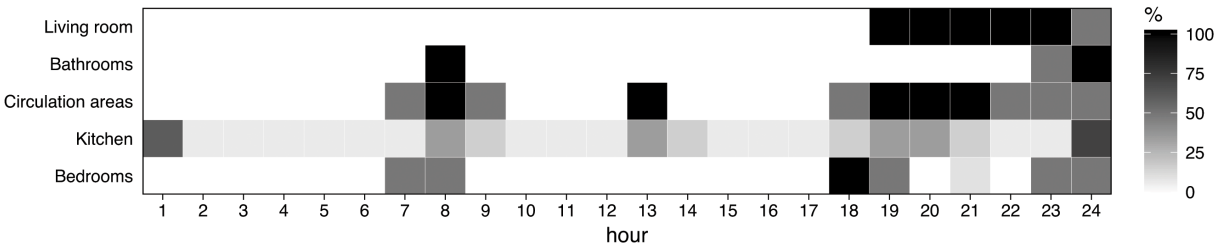

Fig. 3. Electric equipment schedules in each zone.

2.2.3. Weather data

For each thermal mass level, the same sixteen Mediterranean locations were chosen and the corresponding weather data was used – available from the EnergyPlus website [32]. The locations were Venice (Italy, ITA), Marseille (France, FRA), Podgorica (Montenegro, MNE), Istanbul (Turkey, TUR), Naples (ITA), Valencia (Spain, ESP), Izmir (TUR), Athens (Greece, GRC), Tunis (Tunisia, TUN), Algiers (Algeria, DZA), Malaga (ESP), Larnaca (Cyprus, CYP), Casablanca (Morocco, MAR), Tripoli (Libya, LBY), Tel Aviv (Israel, ISR), and Alexandria (Egypt, EGY). According to the Köppen-Geiger World Map climate classification [33], the locations are characterized as being humid subtropical (mild with no dry season and hot summer), except Malaga (ESP), which has a Mediterranean climate (dry hot summer and mild winter), and Tripoli (LBY), which is classified as hot subtropical steppe. More information on the climate locations is described in ref. [27] (latitude, longitude, altitude, and climate type designation).

2.3. Statistical analysis

For each thermal mass level, a synthetic dataset was created with the buildings' geometry data (number of stories, spaces, openings, surface areas of the elements, volumes, and other geometric

information), construction data (the physical properties of transparent and opaque elements), and performance data (electric energy consumption, water consumption, thermal discomfort, and thermal energy production). Each dataset totalizes 192 000 dwellings; *i.e.*, 12 000 buildings per location. These two datasets are publicly available online (see ref. [34] for heavyweight and ref. [35] for lightweight construction types).

With these two thermal-mass-level datasets, a statistical analysis was conducted by splitting each one into groups according to their location and into subgroups according to the thermal transmittance values of their envelope elements. Using the lightweight construction results as reference dataset, the quartiles of each subgroup for total energy demand for air-conditioning, as well as for cooling and heating energy consumptions, were drawn in the form of box and whisker diagrams. The subgroup with the lowest total energy average was determined to find the ideal U-values for transparent and opaque elements in each Mediterranean location. For each subgroup of thermal transmittance values, six geometry-based indexes – building volume (V), shape coefficient ($C_f = S/V$), relative compactness ($RC = 6V^{2/3}/S$), window-to-floor ratio ($WFR = S_{win}/S_{floor}$), window-to-wall ratio ($WWR = S_{win}/S_{wall}$), and window-to-surface ratio ($WSR = S_{win}/S$); where S is the surface area in contact with the outdoor environment, and S_{floor}, S_{win}, and S_{wall} are the floor, window, and wall surface areas, respectively – were correlated with the total energy consumption. As the WSR is better able to capture the impact of the exterior opaque elements and their relation with the window areas [25], this index was extended to each cardinal orientation – WSR-N, WSR-E, WSR-S, and WSR-W, for north, east, south and west orientations, respectively.

Finally, the differences in total energy, cooling energy, and heating energy between the heavyweight and lightweight construction subgroups were calculated, thus allowing to determine the impact of the thermal mass change within the whole thermal transmittance range considered. Additionally, the impact of thermal mass on the building geometry was determined by comparing the standard deviation of each subgroup. In the end, the ideal U-values for each thermal mass level were compared in terms of the energy performance and the geometry impact.

3. Results and Discussion

Figs. 4 and 5 display the results of total energy demand for air-conditioning, cooling (blue boxplots) and heating (red boxplots) energy, and the number of buildings per subgroup of U-values for the dataset of low thermal mass buildings. The x-axis represents the scale of the paired U-values for transparent (top line values) and opaque (bottom line values) elements in the building envelope. The vertical blue line in the total energy graph represents the subgroup of U-values with the lowest average of total energy consumption, thus indicating the energy-ideal U-values for opaque and transparent elements. The locations are sorted from the highest to the lowest latitude,

as presented in section 2.2.3. It is noticeable that for higher U-values the building performance amplitude (*i.e.*, the difference between the maximum and minimum energy consumption) is higher than for lower U-values. This aspect tends to be more evident in higher latitudes. In lower latitudes, the amplitude increases for very low U-values due to an overheating effect of the building. This can be confirmed in the cooling and heating energy boxplots, where for higher latitudes the heating energy demand prevails over the cooling needs, while the opposite occurs for lower latitudes. It is also observable that the ideal U-values (vertical blue line) tend to move further to the right side of the scale as the latitude decreases. However, this relation is strongly dependent on the climate and geographic conditions of each location. These results are also observable for heavyweight construction (see ref. [27] for detailed analysis).

Table 9 presents a comparison of the ideal U-values, for both transparent and opaque elements, between high and low thermal mass constructions. From an energy consumption perspective, with the exception of slightly lower values for lightweight constructions in warmer climates (Valencia – ESP, Larnaca – CYP, Casablanca – MAR, Tripoli – LBY, and Tel Aviv – ISR), no significant difference is found. Alexandria (EGY) is an exception to this trend as it presents higher ideal U-values.

Figs. 6 to 9 depict in the left graphs the correlation (coefficient of determination R^2) between the geometry-based indexes (V – volume; C_f – shape coefficient; RC – relative compactness; WFR – window-to-floor ratio; WWR – window-to-wall ratio; and WSR – window-to-surface ratio) and the energy consumption for air-conditioning of each U-values subgroup for each location. The intervals of the correlation scale for the coefficient of determination (R^2) were defined as: very weak $[0, 0.2[$, weak $[0.2, 0.4[$, moderate $[0.4, 0.6[$, strong $[0.6, 0.8[$, and very strong $[0.8, 1]$. The green color represents a negative correlation and a red color a positive correlation. The geometry-ideal U-values interval is identified in every graph with a blue rectangle, which corresponds to the WSR

Table 9. Ideal U-values (transparent and opaque elements) per location. The lowest U-value of both thermal mass levels is marked in bold.

		High thermal mass				**Low thermal mass**			
		Energy-ideal U-values		**Geometry-ideal U-values**		**Energy-ideal U-values**		**Geometry-ideal U-values)**	
City	**Country**	**Transparent**	**Opaque**	**Transparent**	**Opaque**	**Transparent**	**Opaque**	**Transparent**	**Opaque**
Venice	ITA	0.40	0.10	0.40	0.10	0.40	0.10	0.40	0.10
Marseille	FRA	0.80	0.20	0.80	0.20	0.80	0.20	0.80	0.20
Podgorica	MNE	0.80	0.20	0.60	0.15	0.80	0.20	0.60	0.15
Istanbul	TUR	0.60	0.15	0.60	0.15	0.60	0.15	0.60	0.15
Naples	ITA	1.00	0.25	0.80	0.20	1.00	0.25	**0.60** – 0.80	**0.15** – 0.20
Valencia	ESP	1.40	0.35	1.00 – 1.20	0.25 – 0.30	**1.20**	**0.30**	1.00 – 1.20	0.25 – 0.30
Izmir	TUR	1.00	0.25	0.80	0.20	1.00	0.25	0.80	0.20
Athens	GRC	1.00	0.25	0.80	0.20	1.00	0.25	0.80 – 1.00	0.20 – 0.25
Tunis	TUN	1.40	0.35	1.00 – 1.20	0.25 – 0.30	1.40	0.35	1.00 – 1.20	0.25 – 0.30
Algiers	DZA	1.60	0.40	1.20	0.30	1.60	0.40	**0.80** – 1.20	**0.20** – 0.30
Malaga	ESP	2.20	0.55	1.40 – 1.60	0.35 – 0.40	2.20	0.55	1.40 – 1.80	0.35 – 0.45
Larnaca	CYP	1.80	0.45	0.80 – 1.20	0.20 – 0.30	**1.60**	**0.40**	0.80 – 1.20	0.20 – 0.30
Casablanca	MAR	2.20	0.55	1.80 – 2.00	0.45 – 0.50	**2.00**	**0.50**	**1.60** – 2.00	**0.40** – 0.50
Tripoli	LBY	1.40	0.35	1.00 – 1.20	0.25 – 0.30	**1.20**	**0.30**	**0.60** – **1.00**	**0.15** – **0.25**
Tel Aviv	ISR	2.00	0.50	1.20 – 1.60	0.30 – 0.40	**1.60**	**0.40**	**0.80** – 1.60	**0.20** – 0.40
Alexandria	EGY	**2.60**	**0.65**	1.40 – 2.20	0.35 – 0.55	3.20	0.80	**1.00** – **1.80**	**0.25** – **0.45**

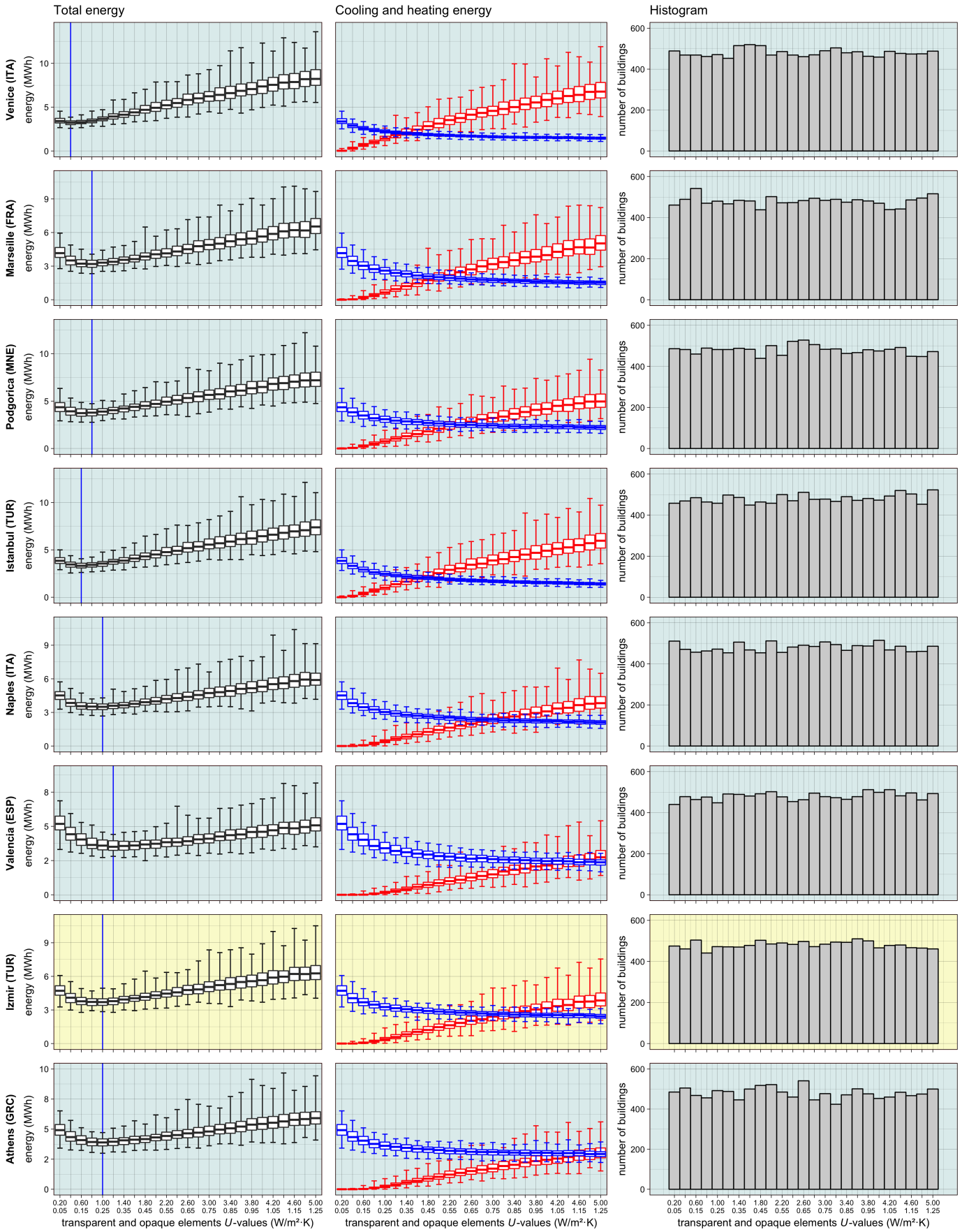

Fig. 4. Total, cooling, and heating energy consumption boxplots and histograms per U-value group per climate location for lightweight construction (part 1/2). Blue boxplots represent cooling energy and red boxplots heating energy. The blue vertical line represents the ideal U-value. The light blue background indicates the locations in Europe, light yellow in Asia, and light red in the African continent.

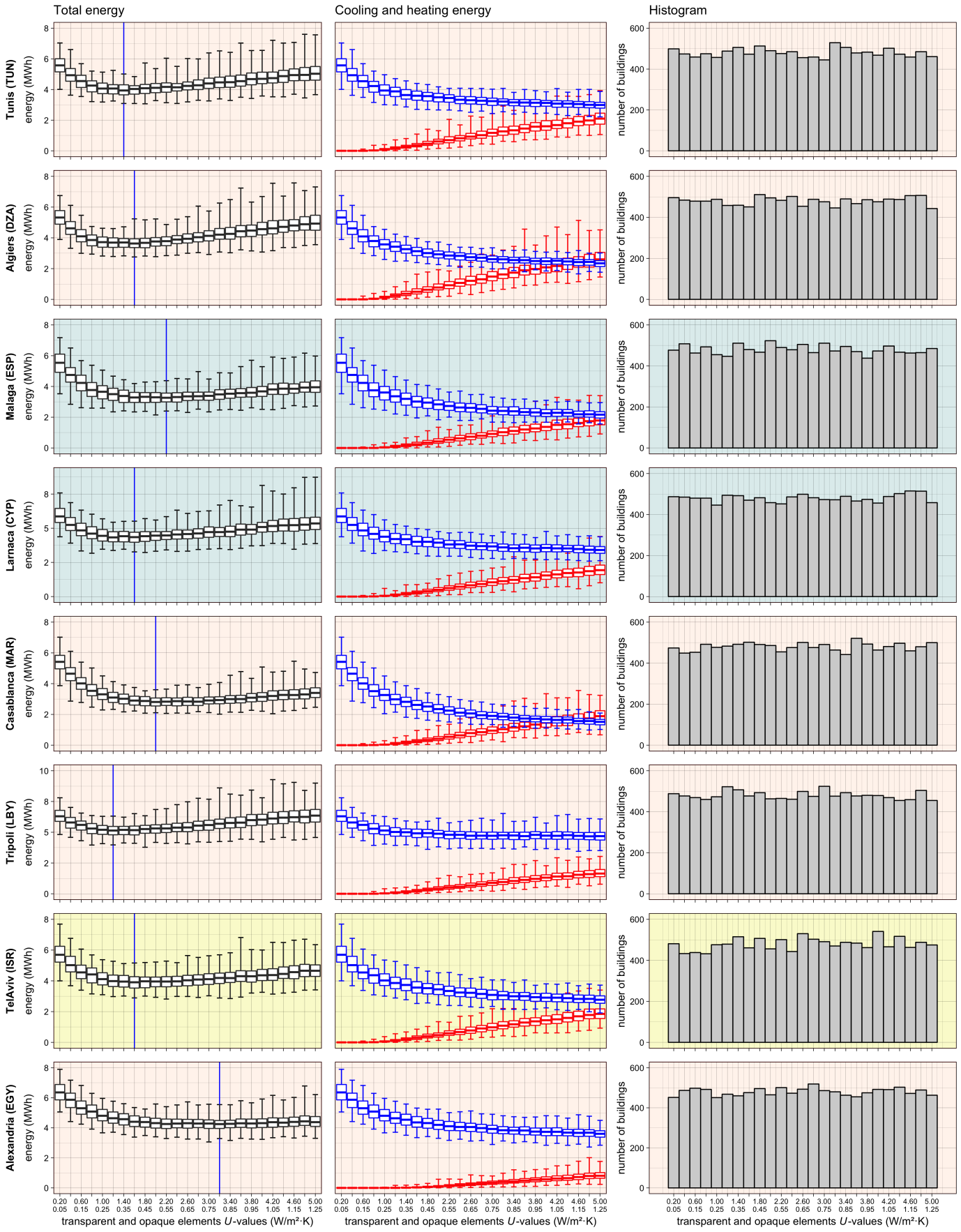

Fig. 5. Total, cooling, and heating energy consumption boxplots and histograms per U-value group per climate location for lightweight construction (part 2/2). Blue boxplots represent cooling energy and red boxplots heating energy. The blue vertical line represents the ideal U-value. The light blue background indicates the locations in Europe, light yellow in Asia, and light red in the African continent.

index with $R^2 \leq 0.02$ or the lowest value. Accordingly, three sections of the building geometry influence can be identified in the graph: to the right of the rectangle, the overall window-based and shape-based indexes have negative correlations and the volume has positive correlation; to the left, the overall window-based and shape-based indexes invert their correlation in comparison to the right side; and, within the blue rectangle, the overall indexes present null or very weak correlations. Therefore, the design guidelines that can be identified are different for each part.

It is noticeable that, as the latitude decreases, the ideal U-value range tends to be higher in the scale and becomes wider, thus meaning that in such intervals building designers are freer to explore new design solutions without compromising the overall energy performance (see ref. [27] for detailed analysis on design guidelines). These results are similar to the ones obtained for the heavyweight construction [27].

On the right side of each figure, the calculated probability (p-value) for the null hypothesis (H_0) is presented with a threshold of 0.01 (values above or equal to this threshold are presented in red gradient background). When compared with the heavyweight construction (Table 9), low thermal mass presents lower and wider intervals of geometry-ideal U-values in warmer climates, such as Naples (ITA), Algiers (DZA), Casablanca (MAR), Tripoli (LBY), Tel Aviv (ISR), and Alexandria (EGY), while in the remaining locations the differences are not significant.

Figs. 10 to 13 illustrate the differences in the total, cooling, and heating energy between heavy- and lightweight construction types for each subgroup of U-values – a positive value denotes higher energy consumption than that of lightweight construction. The maximum and minimum difference values in percentage are also signaled in each graph. The last graph on the right presents the standard deviation (σ) of energy consumption of each U-values subgroup for high (purple) and low (dark green) thermal mass. It can be observed that each thermal mass level and pair of thermal transmittance values result in different energy performances. Generally, a high thermal mass increases the total energy consumption throughout the whole scale of U-values, except for Valencia (ESP), Algiers (DZA), Malaga (ESP), Casablanca (MAR), and Tel Aviv (ISR), which present an increase in energy consumption only for low U-values, and a reduction at the middle and upper parts of the U-values scale, especially in Malaga and Casablanca. For the northern latitudes – Venice (ITA), Marseille (FRA), Podgorica (MNE), and Istanbul (TUR) –, a high thermal mass increases heating energy for the upper part of the U-value scale. In the remaining locations, a high thermal mass contributes positively to a reduction in heating energy.

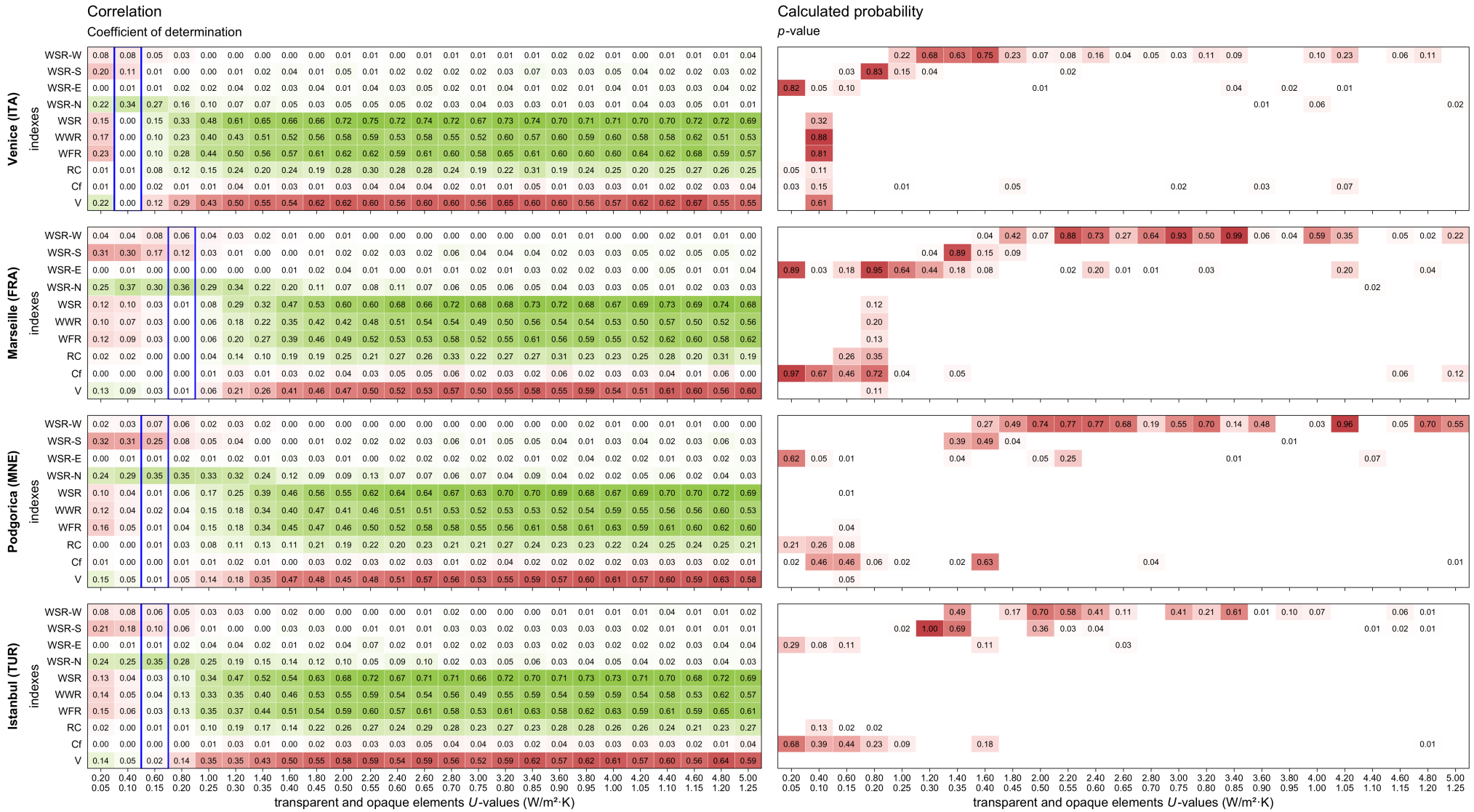

Fig. 6. Correlation of geometry indexes per U-value group per climate location (part 1/4) for low mass construction. In the left graph, green cells show negative correlation and red cells represent positive correlation. The blue rectangle indicates the U-value range for WSR with $R^2 \leq 0.02$ or minimum value. In the right graph, red cells indicate subgroups having p-value above or equal to the threshold of 0.01.

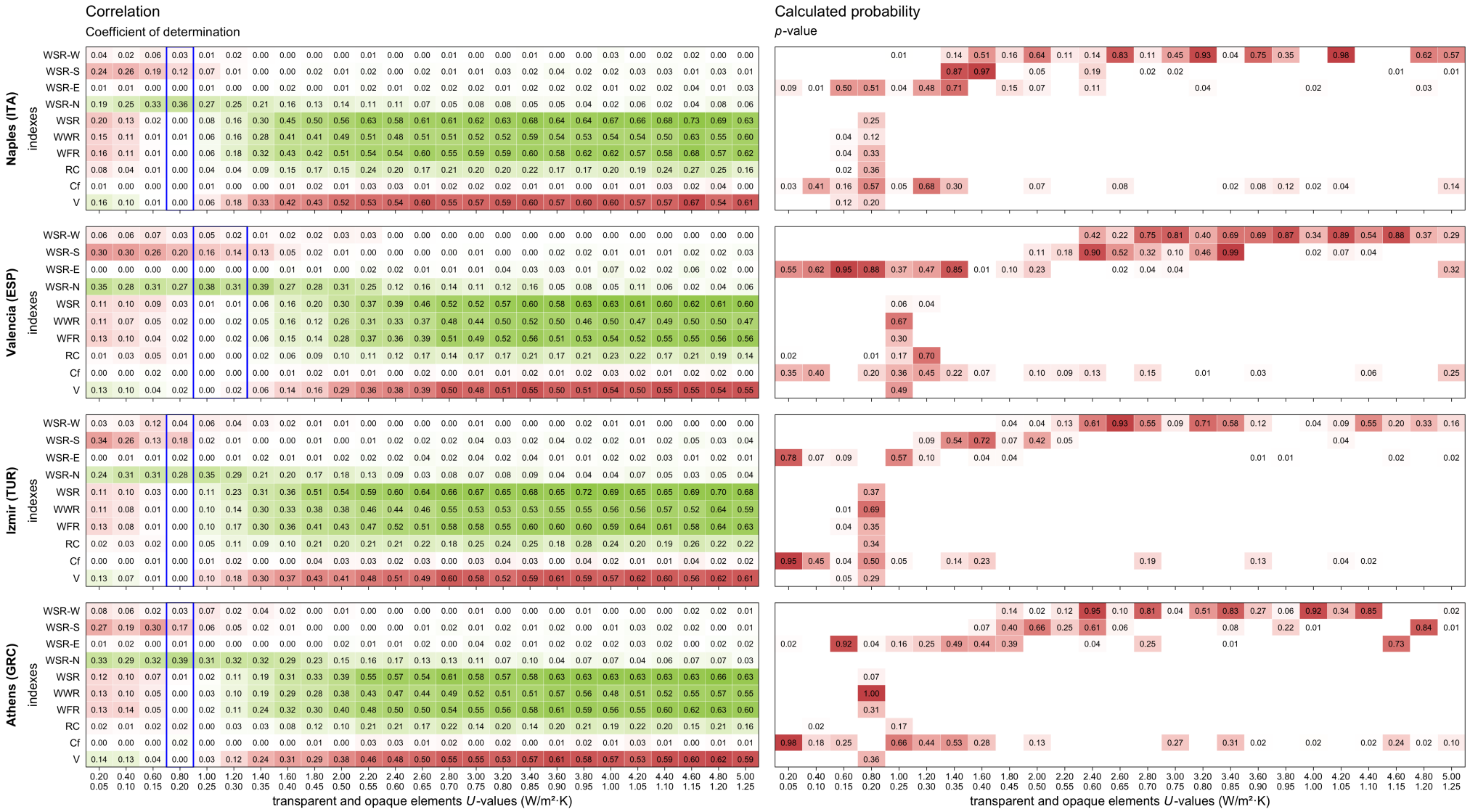

Fig. 7. Correlation of geometry indexes per U-value group per climate location (part 2/4) for low mass construction. In the left graph, green cells show negative correlation and red cells represent positive correlation. The blue rectangle indicates the U-value range for WSR with $R^2 \leq 0.02$ or minimum value. In the right graph, red cells indicate subgroups having p-value above or equal to the threshold of 0.01.

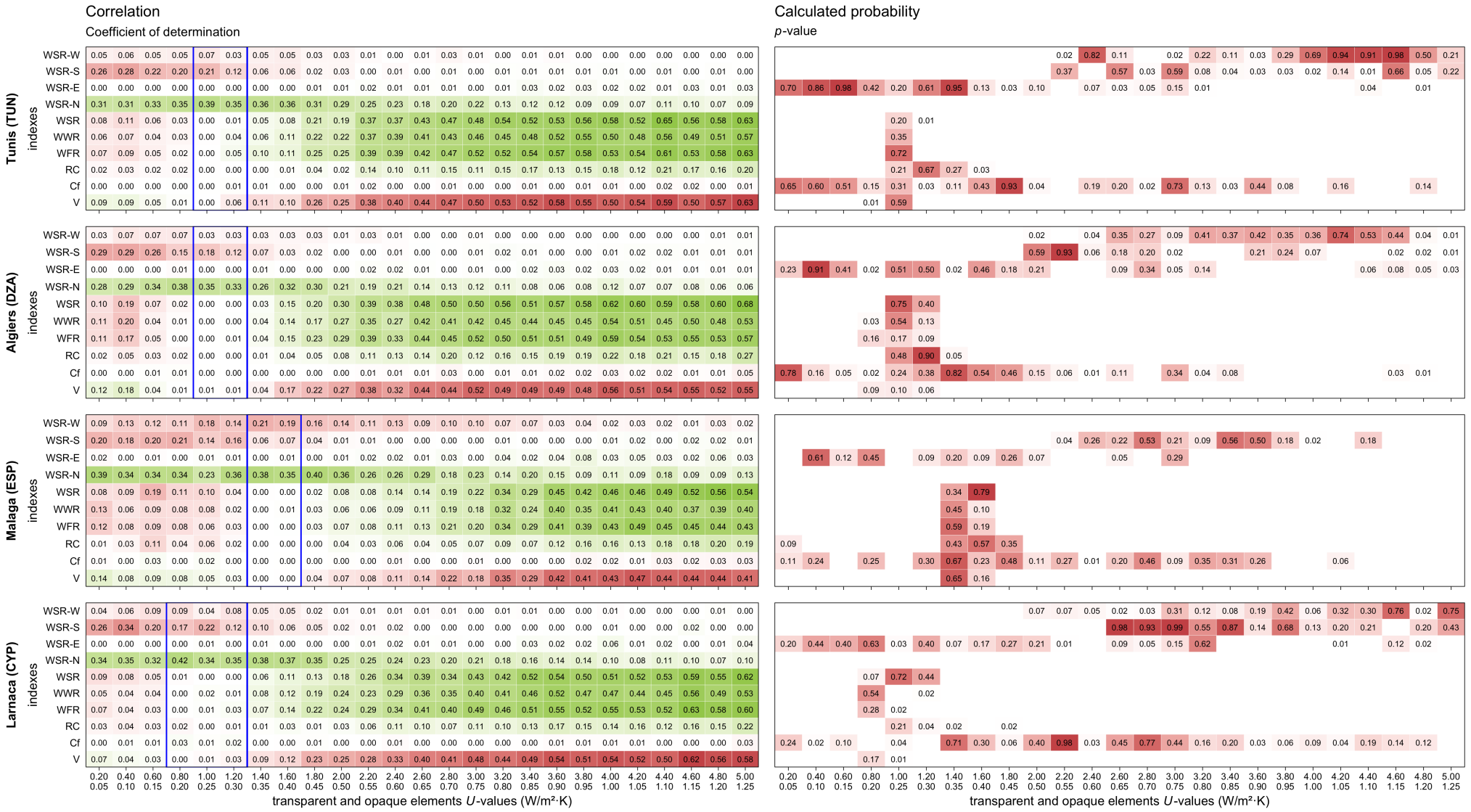

Fig. 8. Correlation of geometry indexes per U-value group per climate location (part 3/4) for low mass construction. In the left graph, green cells show negative correlation and red cells represent positive correlation. The blue rectangle indicates the U-value range for WSR with $R^2 \leq 0.02$ or minimum value. In the right graph, red cells indicate subgroups having p-value above or equal to the threshold of 0.01.

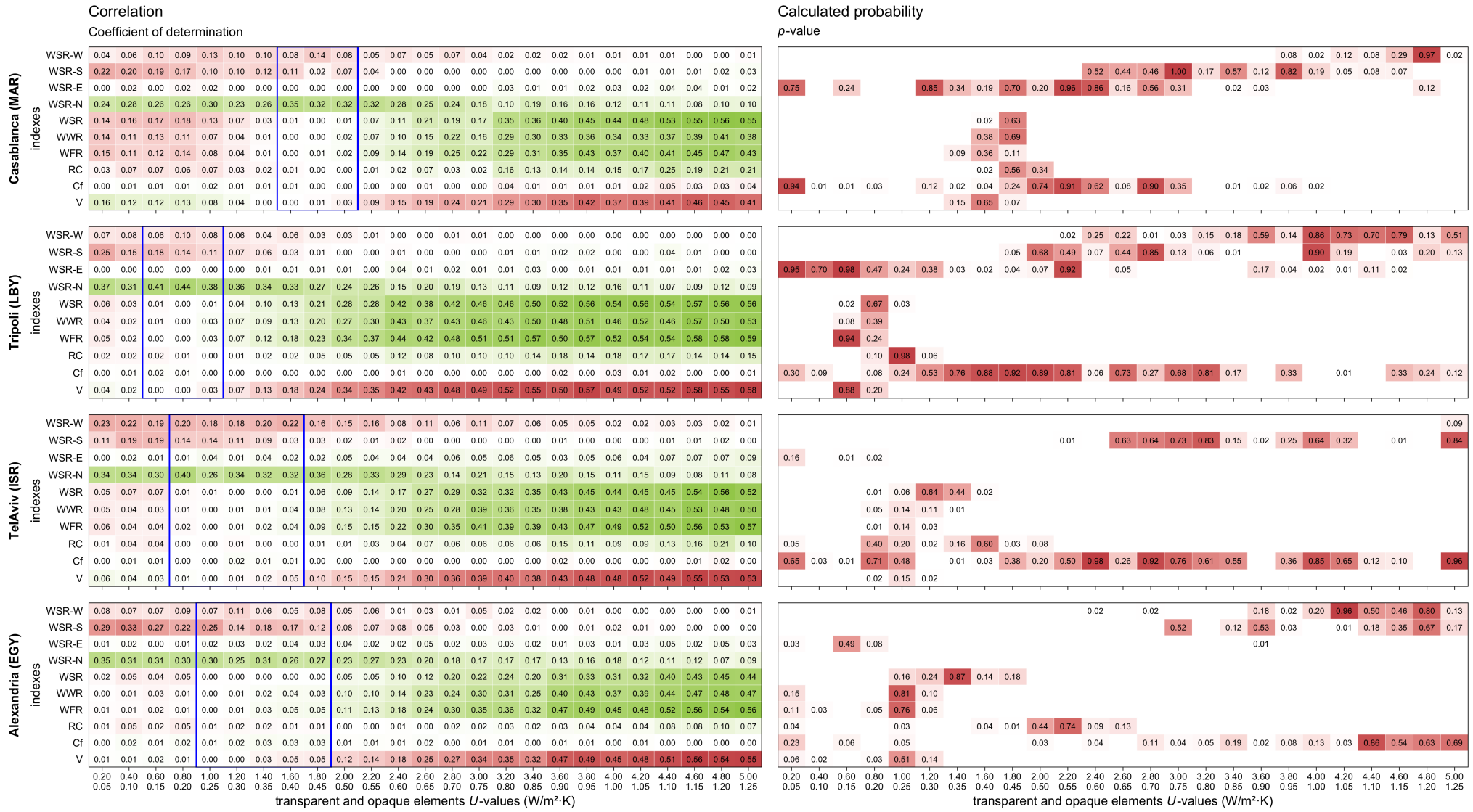

Fig. 9. Correlation of geometry indexes per U-value group per climate location (part 4/4) for low mass construction. In the left graph, green cells show negative correlation and red cells represent positive correlation. The blue rectangle indicates the U-value range for WSR with $R^2 \leq 0.02$ or minimum value. In the right graph, red cells indicate subgroups having p-value above or equal to the threshold of 0.01.

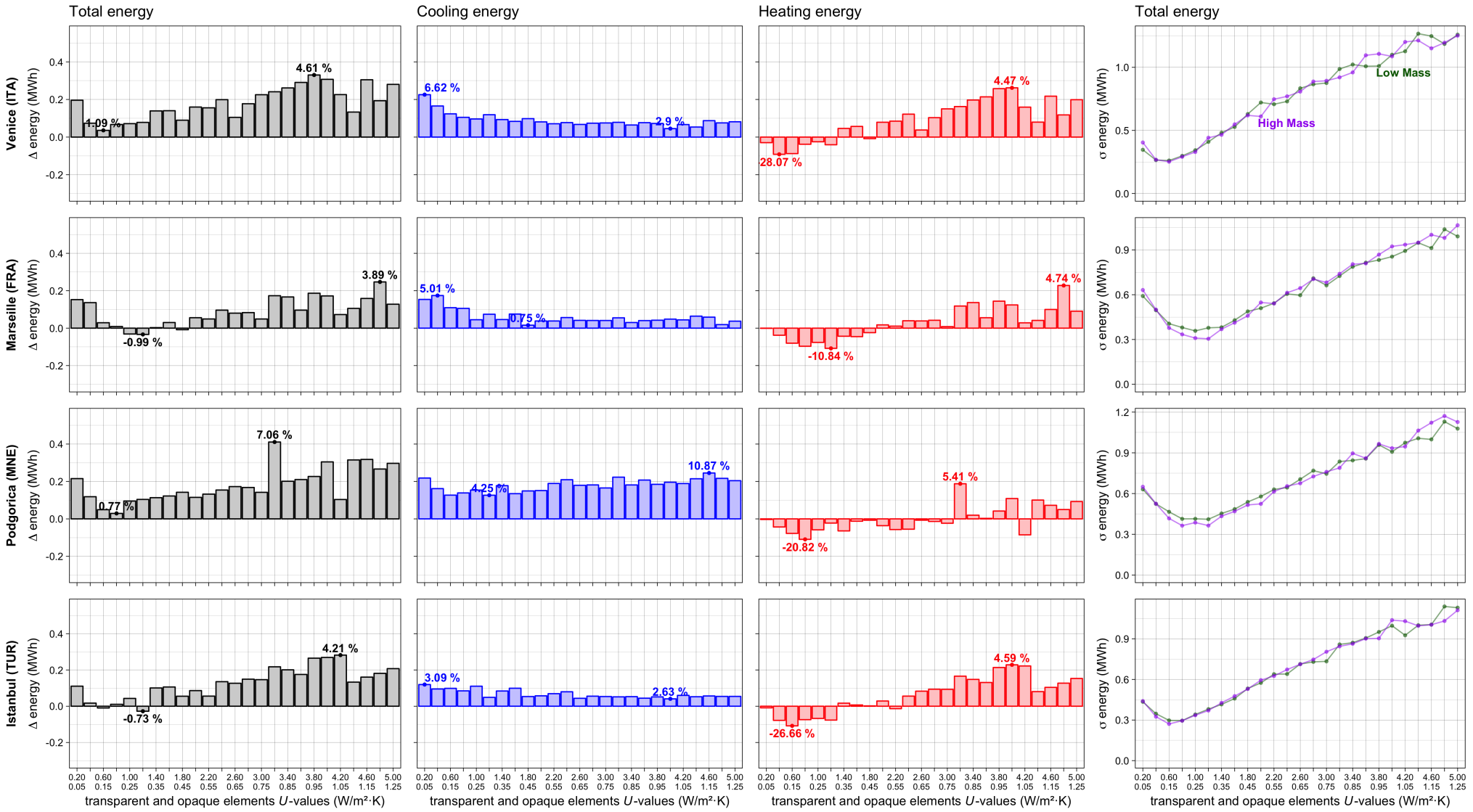

Fig. 10. Differences in total, cooling and heating energy consumptions between heavy- and lightweight construction types per U-value group per climate location; total energy standard deviation (σ) for low mass construction (dark green line) and high mass construction (purple line) per U-value group per climate location (part 1/4). The marked values correspond to the percentage of the max and min difference between the heavy- and lightweight construction types.

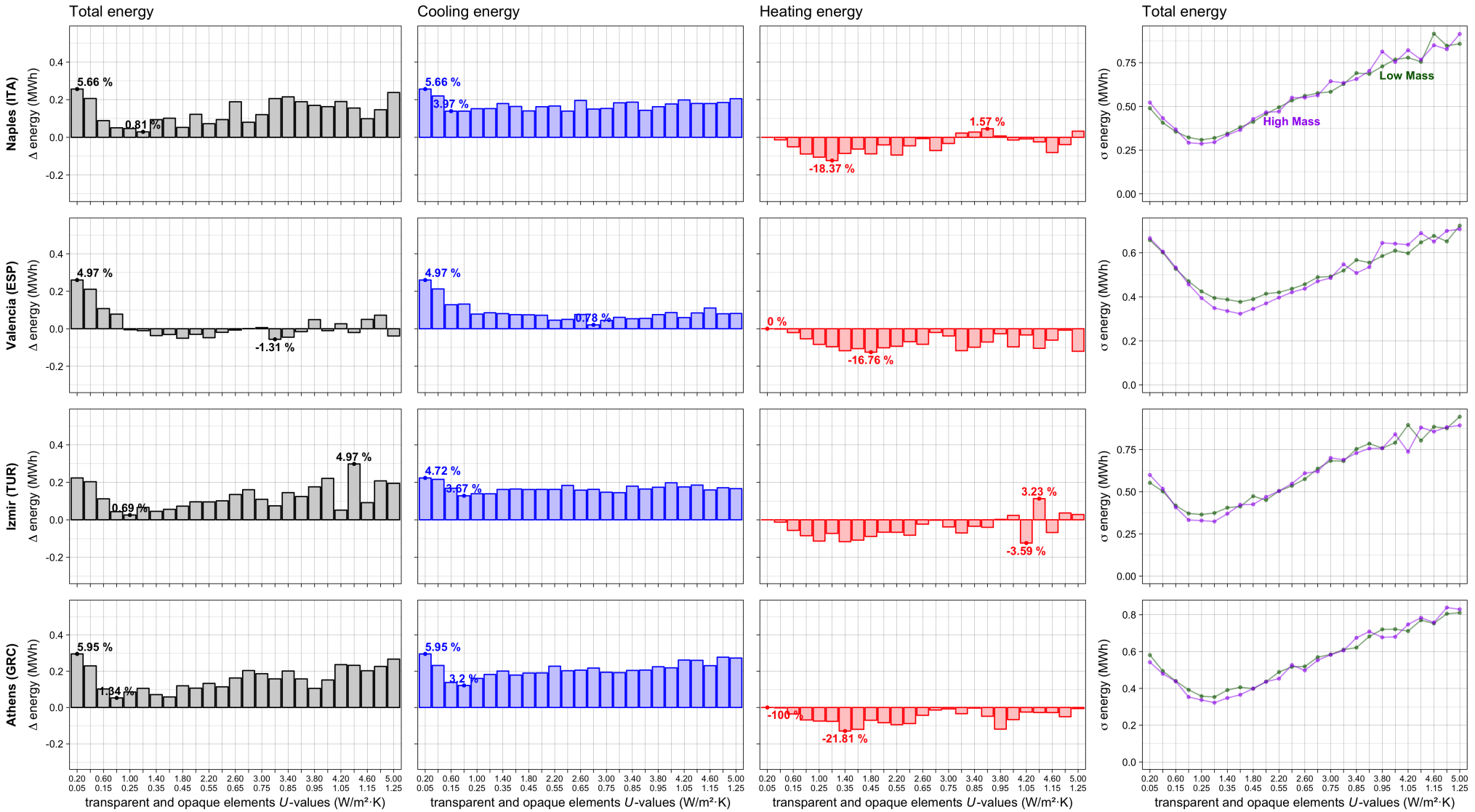

Fig. 11. Differences in total, cooling and heating energy consumptions between heavy- and lightweight construction types per U-value group per climate location; total energy standard deviation (σ) for low mass construction (dark green line) and high mass construction (purple line) per U-value group per climate location (part 2/4). The marked values correspond to the percentage of the max and min difference between the heavy- and lightweight construction types.

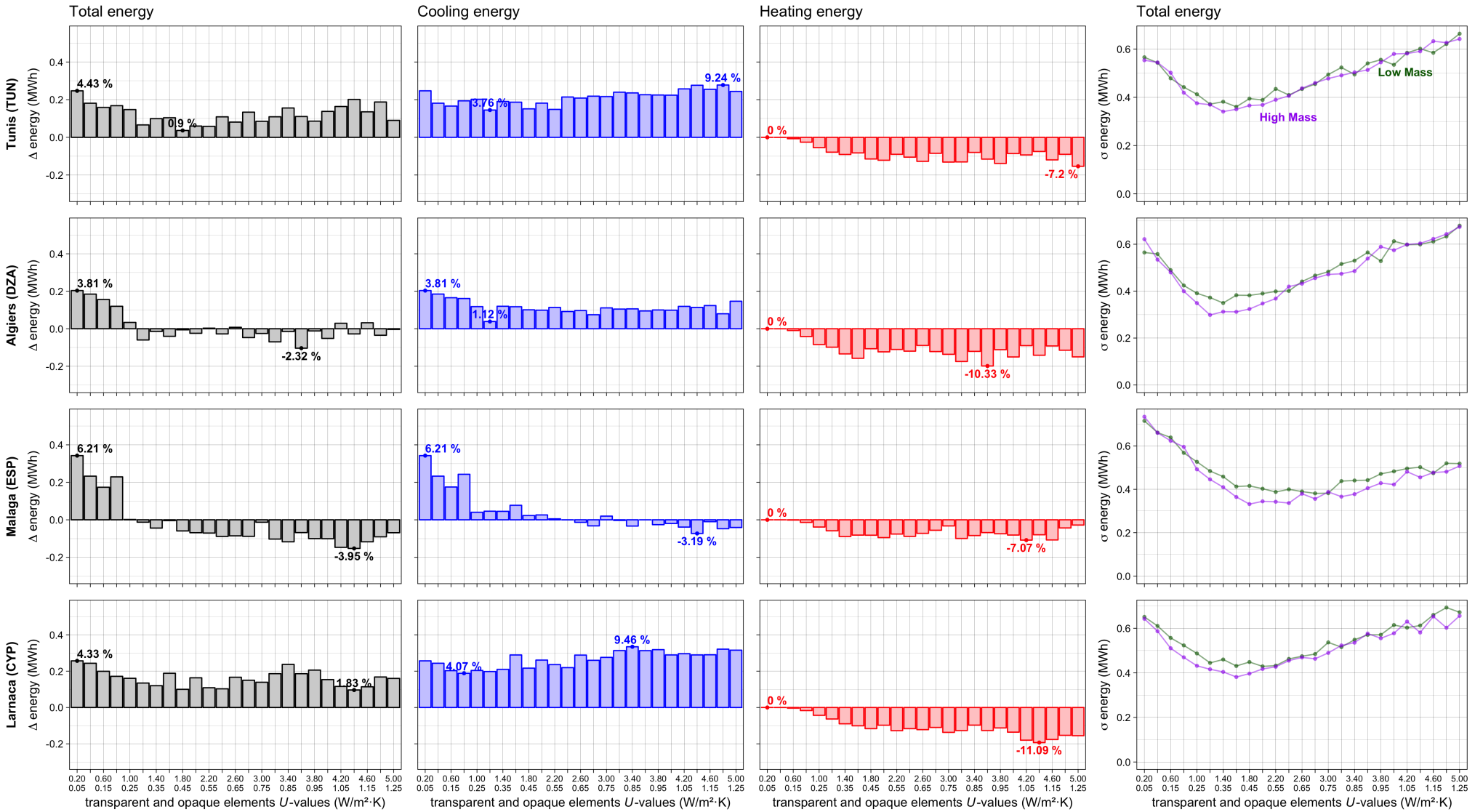

Fig. 12. Differences in total, cooling and heating energy consumptions between heavy- and lightweight construction types per U-value group per climate location; total energy standard deviation (σ) for low mass construction (dark green line) and high mass construction (purple line) per U-value group per climate location (part 3/4). The marked values correspond to the percentage of the max and min difference between the heavy- and lightweight construction types.

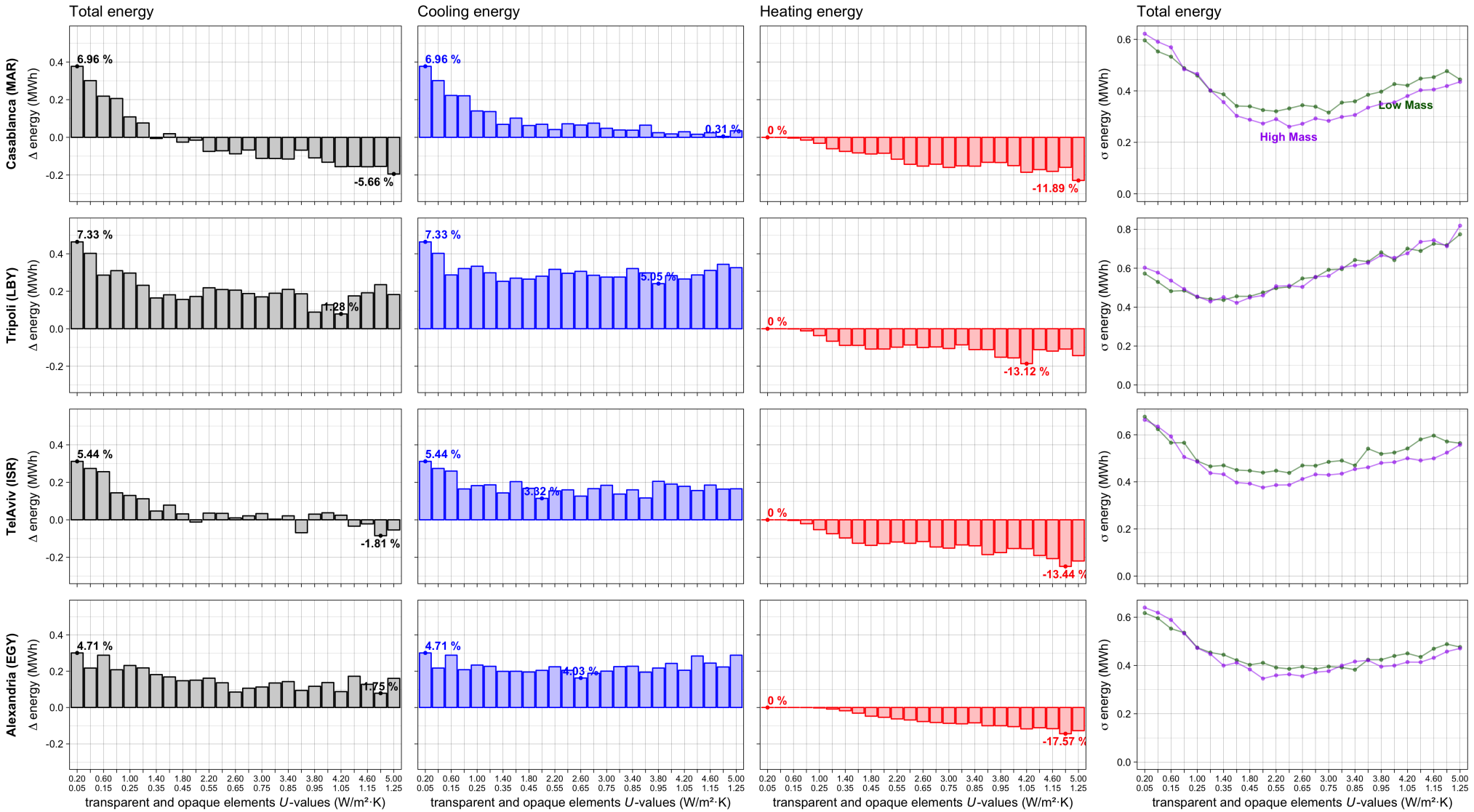

Fig. 13. Differences in total, cooling and heating energy consumptions between heavy- and lightweight construction types per U-value group per climate location; total energy standard deviation (σ) for low mass construction (dark green line) and high mass construction (purple line) per U-value group per climate location (part 4/4). The marked values correspond to the percentage of the max and min difference between the heavy- and lightweight construction types.

In relation to cooling energy, a high thermal mass increases consumption in all locations for all subgroups of U-values (except Malaga – ESP, which only presents such behavior in the initial part of the U-values scale). However, in northern locations, such as Venice (ITA), Marseille (FRA), Podgorica (MNE), and Istanbul (TUR), a high thermal mass worsens energy performance (in comparison with a low thermal mass) for higher U-values, and in southern locations, such as Algiers (DZA), Malaga (ESP), Casablanca (MAR), Tripoli (LBY), Tel Aviv (ISR), and Alexandria (EGY), such effect is noticeable for lower U-values.

Regarding the relative difference between the two thermal mass levels, Tripoli (LBY) presents the highest percentage of total energy increase due to high thermal mass, with 7.33 %, while Casablanca (MAR) presents the largest reduction, with −5.66 %. In the case of cooling energy, Podgorica (MNE) presents an increase of 10.87 % and Malaga (ESP) a decrease of 3.19 %, while, for heating energy, Podgorica (MNE) presents an increase of 5.41 % and Istanbul (TUR) a reduction of 26.66 %.

On the right-hand side of Figs. 10 to 13, the standard deviation graphs show that, for higher latitudes with colder climates, the thermal mass does not affect the influence of the building geometry. However, for southern and warmer climates, there is a tendency for lightweight construction to have a higher standard deviation (*e.g.*, Algiers – DZA, Malaga – ESP, Larnaca – CYP, Casablanca – MAR, Tel Aviv – ISR, and Alexandria – EGY), meaning that, in hotter climates, high thermal mass diminishes the influence of geometry on the buildings' energy performance.

The main findings of this work can be summarized as follows:

- The energy-ideal U-values are very similar for both thermal inertia datasets; however, Valencia (ESP), Larnaca (CYP), Casablanca (MAR), Tripoli (LBY), and Tel Aviv (ISR) have slightly lower ideal U-values for low thermal mass, and Alexandria (EGY) much higher values;

- For lightweight construction, the geometry-ideal U-values have lower and wider intervals, particularly for Naples (ITA), Algiers (DZA), Casablanca (MAR), Tripoli (LBY), Tel Aviv (ISR), and Alexandria (EGY);

- Heavyweight construction results in higher energy consumption throughout the entire U-values scale, except for Valencia (ESP), Algiers (DZA), Malaga (ESP), Casablanca (MAR), and Tel Aviv (ISR), which present an increase in the energy consumption for low U-values and a reduction in the middle and upper parts of the U-values scale;

- Heavyweight construction does not contribute to the reduction of heating energy demand in northern locations; Venice (ITA), Marseille (FRA), Podgorica (MNE), and Istanbul (TUR) present an increase in heating energy consumption in the upper part of the U-values scale;

and,

- High thermal mass contributes to the increase in cooling energy consumption in all locations studied, except in Malaga (ESP), where it only increases in the lowest part of the U-values scale.

4. Conclusion

The comparative statistical analysis of both thermal mass levels allows to confirm the variability of the contribution that thermal mass has on energy consumption for air-conditioning. In other words, the contradictory results found in previous works is not just a consequence of using different methodological approaches, different building types, and different energy systems operations, but rather the outcome of the complex nature of the physical problem at hand. The results demonstrate that the impact of the thermal mass is dependent on the chosen U-value of the building envelope. For example, for the same climate location, low thermal mass can be beneficial if having higher thermal transmittance values, and detrimental when using lower values, such as in Casablanca, which is characterized by having a warm-humid subtropical climate with an all-year high relative humidity; and in other climate locations, such as Istanbul (a warm-marine climate with lower incident solar radiation and dryer summers than Casablanca), higher U-values leads to larger energy consumption in heavyweight construction than in lightweight construction.

Overall, heavyweight construction increases the cooling energy demand and reduces the heating energy demand for the southern and warmer climates, but may increase the heating energy demand for northern and colder climates. It was also concluded that low thermal mass leads to lower energy- and geometry-ideal U-values for southern and warmer locations, and to a wider range of geometry-ideal U-values. This obliges one to think of these thermophysical properties of the building construction elements and on how they relate to the geographic and climatic contexts in a non-linear way.

This type of study allows to detach from the potential bias that may result from using a single building geometry in a specific climatic location to test the effects of different thermophysical properties of the envelope elements on energy performance. The randomness and large datasets of building geometries allow to confidently study the impact of the thermal mass throughout the thermal transmittance scale. However, it should be pointed out that these results are dependent on the studied building types, occupants' behaviors, and systems' operations. Therefore, further studies should complement the present results by analyzing other types of buildings in other operation scenarios.

The inherent characteristics of this work, namely the impossibility of defining the dynamic

properties of the external building construction elements (*e.g.*, using the admittance method of ISO EN 13786) by considering an equivalent thermal mass and randomly assigned U-values, led to the use of thermal mass alone as a rough description of the thermal inertia influence. Therefore, the results of this approach should be seen as general indicators of the most adequate thermal transmittance values for different types of thermal inertia constructions. The results can thus serve as a starting point for further studies aiming to extend this work to specific cases (*e.g.*, specific climate locations and operating scenarios), where thermal inertia may be taken into account using more detailed criteria.

5. Data availability

The dataset related to heavyweight construction buildings located in the sixteen locations in the Mediterranean can be found at URL `https://goo.gl/mfDXCd`, hosted at figshare ([34]).

The dataset related to lightweight construction buildings located in the sixteen locations in the Mediterranean can be found at URL `https://goo.gl/C1NWvN`, hosted at figshare ([35]).

The set of twelve input data files (IDF), to be used in EnergyPlus, having random thermal transmittance can be found at URL `https://bit.ly/2vcLTxg`, hosted at figshare ([31]).

Acknowledgements

The research presented has been developed under the *Energy for Sustainability Initiative* of the University of Coimbra (UC). The authors are grateful to Anabela Alves for proofreading the text.

Funding: This work has been financed by the Portuguese Foundation for Science and Technology (FCT) and by the European Regional Development Fund (FEDER) through COMPETE 2020 – Operational Program for Competitiveness and Internationalization (POCI) in the framework of the research project Ren4EEnIEQ (PTDC/EMS-ENE/3238/2014, POCI-01-0145-FEDER-016760, and LISBOA-01-0145-FEDER-016760) and by project UID/Multi/00308/2019 supported by FCT.

Declarations of interest: none.

References

[1] A. Gagliano, F. Patania, F. Nocera, C. Signorello, Assessment of the dynamic thermal performance of massive buildings, Energy and Buildings 72 (2014) 361–370. doi:10.1016/j.enbuild.2013.12.060.

[2] S. Martín, F. R. Mazarrón, I. Cañas, Study of thermal environment inside rural houses of Navapalos (Spain): The advantages of reuse buildings of high thermal inertia, Construction and Building Materials 24 (2010) 666–676. doi:10.1016/j.conbuildmat.2009.11.002.

[3] J. A. Orosa, A. C. Oliveira, A field study on building inertia and its effects on indoor thermal environment, Renewable Energy 37 (2012) 89–96. doi:10.1016/j.renene.2011.06.009.

[4] R. S. McLeod, C. J. Hopfe, A. Kwan, An investigation into future performance and overheating risks in Passivhaus dwellings, Building and Environment 70 (2013) 189–209. doi:10.1016/j.buildenv.2013.08.024.

[5] F. Stazi, C. Bonfigli, E. Tomassoni, C. Di Perna, P. Munafò, The effect of high thermal insulation on high thermal mass: Is the dynamic behaviour of traditional envelopes in Mediterranean climates still possible?, Energy and Buildings 88 (2015) 367–383. doi:10.1016/j.enbuild.2014.11.056.

[6] S. Verbeke, A. Audenaert, Thermal inertia in buildings: A review of impacts across climate and building use, Renewable and Sustainable Energy Reviews 82 (2017) 2300–2318. doi:10.1016/j.rser.2017.08.083.

[7] N. Aste, A. Angelotti, M. Buzzetti, The influence of the external walls thermal inertia on the energy performance of well insulated buildings, Energy and Buildings 41 (2009) 1181–1187. doi:10.1016/j.enbuild.2009.06.005.

[8] N. Aste, F. Leonforte, M. Manfren, M. Mazzon, Thermal inertia and energy efficiency - Parametric simulation assessment on a calibrated case study, Applied Energy 145 (2015) 111–123. doi:10.1016/j.apenergy.2015.01.084.

[9] F. Stazi, E. Tomassoni, C. Bonfigli, C. Di Perna, Energy, comfort and environmental assessment of different building envelope techniques in a Mediterranean climate with a hot dry summer, Applied Energy 134 (2014) 176–196. doi:10.1016/j.apenergy.2014.08.023.

[10] F. Stazi, G. Ulpiani, M. Pergolini, C. Di Perna, The role of areal heat capacity and decrement factor in case of hyper insulated buildings: An experimental study, Energy and Buildings 176 (2018) 310–324. doi:10.1016/j.enbuild.2018.07.034.

[11] A. Dodoo, L. Gustavsson, R. Sathre, Effect of thermal mass on life cycle primary energy balances of a concrete- and a wood-frame building, Applied Energy 92 (2012) 462–472. doi:10.1016/j.apenergy.2011.11.017.

[12] A. Reilly, O. Kinnane, The impact of thermal mass on building energy consumption, Applied Energy 198 (2017) 108–121. doi:10.1016/j.apenergy.2017.04.024.

[13] K. Gregory, B. Moghtaderi, H. Sugo, A. Page, Effect of thermal mass on the thermal performance of various Australian residential constructions systems, Energy and Buildings 40 (2008) 459–465. doi:10.1016/j.enbuild.2007.04.001.

[14] L. Zhu, R. Hurt, D. Correia, R. Boehm, Detailed energy saving performance analyses on thermal mass walls demonstrated in a zero energy house, Energy and Buildings 41 (2009) 303–310. doi:10.1016/j.enbuild.2008.10.003.

[15] S. A. Al-Sanea, M. F. Zedan, Improving thermal performance of building walls by optimizing insulation layer distribution and thickness for same thermal mass, Applied Energy 88 (2011) 3113–3124. doi:10.1016/j.apenergy.2011.02.036.

[16] S. A. Al-Sanea, M. F. Zedan, S. N. Al-Hussain, Effect of thermal mass on performance of insulated building walls and the concept of energy savings potential, Applied Energy 89 (2012) 430–442. doi:10.1016/j.apenergy.2011.08.009.

[17] F. Leccese, G. Salvadori, F. Asdrubali, P. Gori, Passive thermal behaviour of buildings: Performance of external multi-layered walls and influence of internal walls, Applied Energy 225 (2018) 1078–1089. doi:10.1016/j.apenergy.2018.05.090.

[18] Iso 13786:2017 - thermal performance of building components - dynamic thermal characteristics - calculation methods, 2017. URL: https://www.iso.org/standard/65711.html.

[19] N. Bishara, A. Prada, G. Pernigotto, M. Baratieri, A. Gasparella, Analysis of the measurements reliability in dynamic test of the opaque envelope, in: IV High Performance Buildings Conference at Purdue, At West

Lafayette, Indiana, U.S., 2016.

[20] E. Rodrigues, A. R. Gaspar, Á. Gomes, An evolutionary strategy enhanced with a local search technique for the space allocation problem in architecture, Part 1: Methodology, Computer-Aided Design 45 (2013) 887–897. doi:10.1016/j.cad.2013.01.001.

[21] E. Rodrigues, A. R. Gaspar, Á. Gomes, An evolutionary strategy enhanced with a local search technique for the space allocation problem in architecture, Part 2: Validation and performance tests, Computer-Aided Design 45 (2013) 898–910. doi:10.1016/j.cad.2013.01.003.

[22] E. Rodrigues, A. R. Gaspar, Á. Gomes, An approach to the multi-level space allocation problem in architecture using a hybrid evolutionary technique, Automation in Construction 35 (2013) 482–498. doi:10.1016/j.autcon.2013.06.005.

[23] E. Rodrigues, A. R. Gaspar, Á. Gomes, Automated approach for design generation and thermal assessment of alternative floor plans, Energy and Buildings 81 (2014) 170–181. doi:10.1016/j.enbuild.2014.06.016.

[24] E. Rodrigues, A. R. Gaspar, Á. Gomes, Improving thermal performance of automatically generated floor plans using a geometric variable sequential optimization procedure, Applied Energy 132 (2014) 200–215. doi:10.1016/j.apenergy.2014.06.068.

[25] E. Rodrigues, A. R. Amaral, A. R. Gaspar, Á. Gomes, How reliable are geometry-based building indices as thermal performance indicators?, Energy Conversion and Management 101 (2015) 561–578. doi:10.1016/j.enconman.2015.06.011.

[26] E. Rodrigues, M. S. Fernandes, N. Soares, Á. Gomes, A. R. Gaspar, J. J. Costa, The potential impact of low thermal transmittance construction on the European design guidelines of residential buildings, Energy and Buildings 178 (2018) 379–390. doi:10.1016/j.enbuild.2018.08.009.

[27] M. S. Fernandes, E. Rodrigues, A. R. Gaspar, J. J. Costa, Á. Gomes, The impact of thermal transmittance variation on building design in the Mediterranean region, Applied Energy 239 (2019) 581–597. doi:10.1016/j.apenergy.2019.01.239.

[28] E. Rodrigues, N. Soares, M. S. Fernandes, A. R. Gaspar, Á. Gomes, J. J. Costa, An integrated energy performance-driven generative design methodology to foster modular lightweight steel framed dwellings in hot climates, Energy for Sustainable Development 44 (2018) 21–36. doi:10.1016/j.esd.2018.02.006.

[29] F. Stazi (Ed.), Appendix B - Details on Numerical Methods, Butterworth-Heinemann, 2017, pp. 331 – 346. doi:10.1016/B978-0-12-813970-7.00018-2.

[30] EnergyPlus Version 8.8 Documentation: Input Output Reference Manual, Technical Report, U.S. Department of Energy, 2017. URL: https://energyplus.net.

[31] E. Rodrigues, M. S. Fernandes, A. R. Gaspar, Á. Gomes, J. J. Costa, Fileset of twelve energyplus input data files with random thermophysical properties, 2019. URL: https://bit.ly/2vcLTxg. doi:10.6084/m9.figshare.8009555.

[32] Energyplus, 2017. URL: https://energyplus.net.

[33] M. Kottek, J. Grieser, C. Beck, B. Rudolf, F. Rubel, World Map of the Köppen-Geiger climate classification updated, Meteorologische Zeitschrift 15 (2006) 259–263. doi:10.1127/0941-2948/2006/0130.

[34] E. Rodrigues, M. S. Fernandes, A. R. Gaspar, Á. Gomes, J. J. Costa, Dataset of high thermal inertia residential buildings in sixteen mediterranean locations, 2018. URL: https://goo.gl/mfDXCd. doi:10.6084/m9.figshare.5732241.

[35] E. Rodrigues, M. S. Fernandes, A. R. Gaspar, Á. Gomes, J. J. Costa, Dataset of low thermal inertia residential buildings in sixteen mediterranean locations, 2018. URL: https://goo.gl/C1NWvN. doi:10.6084/m9.figshare.6025172.